

Separation of Radiogallium from Zinc Using Membrane-Based Liquid-Liquid Extraction in Flow: Experimental and COSMO-RS Studies

Kristina Søborg Pedersen, Karin Michaelsen Nielsen, Jesper Fonslet, Mikael Jensen & Fedor Zhuravlev

To cite this article: Kristina Søborg Pedersen, Karin Michaelsen Nielsen, Jesper Fonslet, Mikael Jensen & Fedor Zhuravlev (2019) Separation of Radiogallium from Zinc Using Membrane-Based Liquid-Liquid Extraction in Flow: Experimental and COSMO-RS Studies, Solvent Extraction and Ion Exchange, 37:5, 376-391, DOI: [10.1080/07366299.2019.1646982](https://doi.org/10.1080/07366299.2019.1646982)

To link to this article: <https://doi.org/10.1080/07366299.2019.1646982>



© 2019 The Author(s). Published with license by Taylor & Francis Group, LLC.



[View supplementary material](#)



Published online: 05 Aug 2019.



[Submit your article to this journal](#)



Article views: 787



[View related articles](#)



[View Crossmark data](#)



Citing articles: 4 [View citing articles](#)

Separation of Radiogallium from Zinc Using Membrane-Based Liquid-Liquid Extraction in Flow: Experimental and COSMO-RS Studies

Kristina Søborg Pedersen^a, Karin Michaelsen Nielsen^a, Jesper Fonslet^{a,b}, Mikael Jensen^a, and Fedor Zhuravlev^a

^aHevesy Laboratory, Center for Nuclear Technologies, Technical University of Denmark, Roskilde, Denmark; ^bMinerva Imaging ApS, Copenhagen N, Denmark

ABSTRACT



A switch from batch to continuous manufacturing of gallium-68 (⁶⁸Ga) and ⁶⁸Ga-labeled pharmaceuticals can be advantageous, as it recycles isotopically-enriched zinc-68 (⁶⁸Zn), removes pre- and post-irradiation target manipulations, and provides scalability via dose-on-demand production. Herein we report efficient extraction of radiogallium (^{66,67,68}Ga = *Ga) from ZnCl₂/HCl solutions in batch and in flow using a membrane-based liquid-liquid separator. From 5.6 M ZnCl₂/3 M HCl, a 1/2 (v/v) diisopropyl ether (i-Pr₂O)/trifluorotoluene (TFT) solvent extracts 76.3 ± 1.9% of *Ga and 1.9 ± 1.6% of Zn in flow using a single pass through. From 1 M ZnCl₂/6 M HCl, a 1/2 (v/v) *n*-butyl methyl ether (*n*-BuOMe)/TFT solvent extracts 95.7 ± 2.0% of *Ga and 0.005 ± 0.003% of Zn in flow. TFT plays a key role in controlling the interfacial tension between the aqueous and the organic phases, ensuring clean membrane-based separation. The process did not extract Cu, Mn, and Co but did extract Fe. Using HgCl₄ and ZnCl₂ as the extractable species, the COSMO-RS theory predicts the solvation-driven extraction of Ga and Zn with a mean unsigned error of prediction of 4.0% and 3.4% respectively.

KEYWORDS

Gallium-68; gallium-67; liquid-liquid extraction in flow; COSMO-RS

Introduction

Radiogallium (^{66,67,68}Ga = *Ga) has a long and notable history in nuclear medicine. For years, gallium-67 (⁶⁷Ga, *t*_{1/2} = 78 h) scintigraphy has been a linchpin of molecular imaging of cancer,^[1] including non-Hodgkin's lymphoma, Hodgkin's disease,^[2] as well as various infections.^[3] The advancement of positron emission tomography (PET) and FDA's approval of [⁶⁸Ga]Ga-DOTA-TATE (Netspot[®]) moved gallium-68 (⁶⁸Ga, *t*_{1/2} = 68 min) to the forefront of neuroendocrine tumor diagnostics.^[4] In recent years [⁶⁸Ga]Ga-HBED-PSMA-11, a ⁶⁸Ga-labeled PSMA (prostate-specific membrane antigen) ligand emerged as the gold standard for prostate cancer diagnostics, driving a high adoption rate of ⁶⁸Ga in clinics.^[5] The easy chelation chemistry and convenience of ⁶⁸Ge/⁶⁸Ga-generators further contribute to ⁶⁸Ga popularity in clinical and pre-clinical settings.^[6] Meeting the growing demand for ⁶⁸Ga is a challenge, as it is mostly supplied by the gallium generators which suffer from high prices, long lead time, quality inconsistencies, and limited shelf life.^[7] An alternative method of ⁶⁸Ga production is the irradiation of ⁶⁸Zn using a cyclotron.^[8] Since many PET-centers have their own cyclotrons, this is potentially a convenient means of in-house production of ⁶⁸Ga-tracers. However, the cyclotron production of ⁶⁸Ga in solid targets from ⁶⁸Zn

CONTACT Fedor Zhuravlev  fezh@dtu.dk  Center for Nuclear Technologies, Technical University of Denmark, Frederiksborgvej 399, Building 202, 4000 Roskilde, Denmark

Color versions of one or more of the figures in the article can be found online at www.tandfonline.com/isei.

© 2019 The Author(s). Published with license by Taylor & Francis Group, LLC.

This is an Open Access article distributed under the terms of the Creative Commons Attribution-NonCommercial-NoDerivatives License (<http://creativecommons.org/licenses/by-nc-nd/4.0/>), which permits non-commercial re-use, distribution, and reproduction in any medium, provided the original work is properly cited, and is not altered, transformed, or built upon in any way.

and its subsequent separation require either installation of expensive automated solid target systems or requires a series of manual pre- and post-irradiation target handlings. Recently, the production of ^{68}Ga in liquid targets from enriched ^{68}Zn salt solutions has been described, using either $[\text{}^{68}\text{Zn}]\text{ZnCl}_2$ [9,10] or $[\text{}^{68}\text{Zn}]\text{Zn}(\text{NO}_3)_2$. [11–13] Compared to the solid target production, the solution target approach leads to lower radionuclide yields but has an advantage of being more amenable to automation. Currently, all ^{68}Ga made in cyclotron solution targets is produced in batch mode; the desired radionuclide is subsequently purified from the ^{68}Zn salt solution by solid-phase extraction (SPE) using commercial radiosynthesis modules, without directly recycling the ^{68}Zn . If recycling of isotopically enriched ^{68}Zn target material is desired, reprocessing needs to be performed in a separate step.

At the outset, we recognized that the cyclotron production of radiogallium in a solution target is compatible with fluidic chemistry. By coupling a liquid target-based radionuclide production step with a liquid-liquid extraction (LLE) and a phase separation step one can conceivably construct a closed-loop system for continuous manufacturing of ^{68}Ga (Figure 1).

This provides an opportunity to continuously recycle isotopically-enriched ^{68}Zn . We have recently described an efficient LLE in flow of radioisotope titanium-45 (^{45}Ti), where we used a static mixer and a membrane separator with integrated pressure control [14] to extract the ^{45}Ti radionuclide into the organic phase and separate it from the 12 M HCl feed containing scandium-45. [15] By implementing a similar technique here, one can envision a continuous production of ^{68}Ga on the cyclotron through the $^{68}\text{Zn}(p,n)^{68}\text{Ga}$ nuclear reaction using a liquid target with a ^{68}Zn salt solution (Figure 1). After irradiation, the aqueous target solution is combined with the organic extractant, and before entering a membrane separator, the aqueous and organic phases are thoroughly mixed via static mixers and a slug flow developing in the mixing tubing, further facilitating the liquid-liquid extraction. [16] In the separator, the aqueous phase containing ^{68}Zn is retained by the hydrophobic membrane and can be re-routed back into the cyclotron target cell via a closed loop. The organic phase enriched with ^{68}Ga permeates through the membrane, and the radionuclide can be back-extracted (stripped) into 0.1 M HCl, delivering aqueous $[\text{}^{68}\text{Ga}]\text{GaCl}_3$ for radiolabeling.

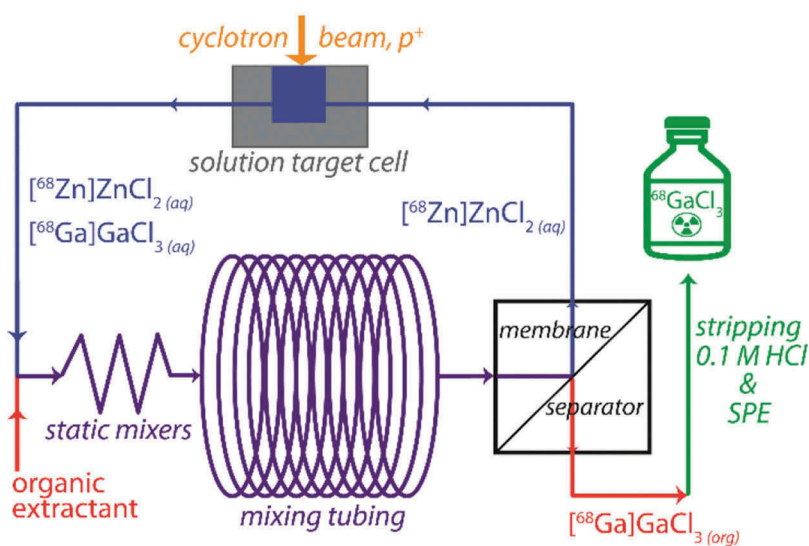


Figure 1. A schematic depicting a conceptual apparatus for continuous production of ^{68}Ga using the $^{68}\text{Zn}(p,n)^{68}\text{Ga}$ nuclear reaction in a cyclotron solution target. Fluidically, the target is coupled to the ^{68}Ga -separation step consisting of liquid-liquid extraction of ^{68}Ga into the organic phase followed by back-extraction (stripping) into 0.1 M HCl. The aqueous phase, containing ^{68}Zn is returned into the cyclotron solution target for irradiation.

The long-term goal of our program is to develop a continuous and automated production of PET radiometals by integrating modern fluidic techniques and process analytical technology tools (PAT) into cyclotron liquid targetry. In this contribution, we present a proof-of-concept study, where we focused on developing an efficient chemical system for in-flow separation of Ga from Zn by evaluating a number of extractants and diluents at different concentration of ZnCl_2 and HCl used in the ^{68}Ga liquid target production. The performance of the optimized extraction system was discussed in a context of Ga/Zn extraction efficiency in batch and flow, initial Zn and HCl concentration, phase cross-contamination, and cyclotron solution target integration. We also present a predictive computational model describing the solution equilibrium for the relevant Ga and Zn species as they partition between the aqueous and organic phases.

Experimental

Materials

Anisole, diethyl ether (Et_2O , b.p. = 35°C , $\log P = .87$), *n*-butyl methyl ether (*n*-BuOMe, b.p. = 70°C , $\log P = 1.54$), tetrahydropyran (THP, b.p. = 88°C , $\log P = .95$), α,α,α -trifluorotoluene (TFT), toluene, 1,2-dichloroethane (DCE), multi-element standard solution 1 for ICP (TraceCert in 10% HNO_3), citric acid, ZnCl_2 , and FeCl_3 , were reagent grade and purchased from Sigma Aldrich. *n*-Dibutyl ether (*n*-Bu₂O, b.p. = 141°C , $\log P = 2.99$) and diisopropyl ether ($^i\text{Pr}_2\text{O}$, b.p. = 69°C , $\log P = 1.49$) were purchased from Merck. Heptane was purchased from VWR Chemicals. *n*-Hexyl methyl ether (*n*-HexOMe, b.p. = 125°C , $\log P = 2.21$) and *n*-amyl ether (*n*-Am₂O, b.p. = 187°C , $\log P = 3.38$) were purchased from abcr GmbH. High purity hydrochloric acid (37%, trace metal basis) from Honeywell was used. All purchased chemicals were used without further purification. Zinc foil (250 μm , 99.9% trace metals basis) and copper foil (500 μm , 99.98% trace metal basis) were purchased from Sigma Aldrich. TK200 resin was purchased from TrisKem. Pall PTFE membranes were used for all experiments; perfluoroalkoxy alkane (PFA) diaphragms were purchased from McMaster Carr. All PFA tubing was purchased from Idex Health and Science. PTFE static mixers were purchased from Stamixco. The 15 mL plastic centrifuge tubes with screw caps (SuperClear) were purchased from VWR. The 10 mL and 25 mL Hamilton glass syringes were purchased from Sigma Aldrich.

Radionuclide production and separation

The radionuclides zinc-65 (^{65}Zn , $t_{1/2}$: 244 d) and ^{67}Ga were used to quantify the Zn and Ga extraction. The radionuclides were produced on a GE 16.5 MeV PETtrace cyclotron by the $^{nat}\text{Cu}(p,n)^{65,63}\text{Zn}$ and $^{nat}\text{Zn}(p,n)^{66,67,68}\text{Ga}$ nuclear reactions, respectively, using a solid target with stacked zinc (250 μm , 750–831 mg) and copper (500 μm , 301–341 mg) foils. The target was irradiated for 120–160 minutes at 10 μA . Subsequently, the target was allowed to decay for at least 18–24 h before further handling to minimize the amount of the co-produced shorter-lived radionuclides ^{63}Zn ($t_{1/2}$ 38 min), ^{68}Ga ($t_{1/2}$ 68 min), and gallium-66 ($t_{1/2}$ 9.5 h). The zinc foil containing around 50 MBq of ^{67}Ga at end of bombardment was dissolved in 3 mL of conc. HCl, and the concentration of HCl was adjusted to 3 M or 6 M. 10–50 μL of this solution was then added per mL to the stock solution of ZnCl_2 also prepared in 3 M or 6 M hydrochloric acid, resulting in an activity concentration of 100–300 kBq/mL (^{67}Ga). The copper foil, containing around 5–10 MBq of ^{65}Zn at end of bombardment, was dissolved in 1.7 mL of concentrated HNO_3 at 60°C . The deep blue solution was evaporated to dryness at 150°C using vigorous argon flow. The blue solid was re-dissolved in 2.5 mL of 1 M HCl and loaded onto TK200 resin (3 g). The resin was washed with 1 M HCl, which removed all the copper (a total of 14 mL), and then with water, which eluted the ^{65}Zn (a total of 25 mL). The fractions containing the highest amount of ^{65}Zn were collected, the solution was evaporated to dryness, dissolved in 2 mL 3 M hydrochloric acid, and added (10–20 μL per mL) to the 5.6 M or 1 M ZnCl_2 stock solution containing the gallium radionuclides. The resulting

solution, containing 100–300 kBq/mL of both ^{67}Ga and ^{65}Zn , simulating a cyclotron-irradiated liquid target mixture was used as the aqueous phase for the LLE. To quantify Cu, Mn, and Co, we used the ^{64}Cu , ^{54}Mn , and ^{60}Co radionuclides, respectively. These were provided by Prof. Xiaolin Hou, except for ^{64}Cu , which was supplied from the medical production at our site using the GE PETtrace cyclotron.

Instrumentation and methods

Ga and Zn were quantified by gamma spectroscopy of the ^{67}Ga and ^{65}Zn using a Princeton Gammatech LGC 5 or Ortec GMX 35195-P germanium detector, calibrated using certified barium-133 and europium-152 sources. The same instrumentation was used to measure activities from ^{64}Cu , ^{54}Mn , and ^{60}Co . An Eppendorf 5702 centrifuge was used to assist in phase separation. Fe was quantified using a Thermo Scientific iCAP 6000 Series ICP Optical Emission Spectrometer. The membrane separator module was purchased from Zaiput Flow Technologies. All experiments used 0.2 μm membrane pore size, 0.002" (0.051 mm) diaphragm, two 10-element static mixers, and 108 cm mixing tube. The solutions for the continuous membrane-based separation were pumped using KDS 100 Legacy Syringe pumps. For batch experiments, the phase mixing was performed using an IKA ROCKER 3D digital shaker. The quantitative NMR (qNMR) was performed on an Agilent 400 MR spectrometer operating at 400.445 MHz (^1H) as described elsewhere.^[17]

Phase equilibrium and liquid-liquid extraction of Ga and Zn in 5.6 M ZnCl_2/HCl – Et_2O system

For the phase equilibrium studies (Figure 4 A), nine centrifuge tubes were each charged with 3 mL of 5.6 M ZnCl_2 made in 0, 0.5, 1, 1.5, 2, 2.5, 3, 3.5, or 4 M HCl solution, respectively, and subsequently 3 mL of Et_2O (pre-saturated with the HCl solution of the corresponding strength) was added. The mixture was shaken for 30 minutes and centrifuged at 4000 rpm to separate the phases. The level of the two phases was marked on the centrifuge tubes with a pen, and the tubes were emptied and dried. Water was added up to the marks and weighted to calculate the volume of the organic and aqueous phase after the mixing. For the LLE studies (Figure 4 B) five centrifuge tubes were each charged with 1.3 mL of 5.6 M ZnCl_2 – made in 0.05, 0.6, 1, 2, or 3 M HCl solution, respectively, also containing ^{67}Ga and ^{65}Zn radionuclides and mixed with 1.3 mL of HCl-saturated Et_2O for 30 minutes. The phases were separated after being centrifuged at 4000 rpm. The activity of ^{67}Ga and ^{65}Zn in the aqueous and in the organic phases were measured by gamma spectroscopy.

Phase separation: diluent study

The 6 M HCl and 3 M HCl solutions used for the experiments were made by diluting concentrated HCl with D_2O . A 1.3 mL 5.6 M ZnCl_2 in 6 M HCl solution was added to each of seven centrifuge tubes. The level of the solution in the centrifuge tubes at upright position was marked with a pen. A 1 mL aliquot of one of the seven ethers, Et_2O , $i\text{Pr}_2\text{O}$, THP, $n\text{-Bu}_2\text{O}$, $n\text{-BuOMe}$, $n\text{-HexOMe}$ or $n\text{-Am}_2\text{O}$, was added to the tubes. After shaking the tubes for one minute, the aqueous and the ether phases became partially or completely miscible. Then, toluene was added to the tubes as a diluent to increase the phase separation between the aqueous and the organic phase. Toluene was added until the aqueous phase had the same volume as before the mixing with ether, which was noted by comparing the level of the aqueous phase with the mark on the tube. The same procedure was used to test different diluents, where 1.3 mL of 5.6 M ZnCl_2 in 6 M HCl solution was added to each of four centrifuge tubes and 1 mL THP was added to each tube. One of four different diluents, anisole, DCE, TFT, or heptane, was added to the tubes until the volume of the aqueous phase was the same as before the mixing. This study with THP and the same diluents as well as toluene was repeated with a 5.6 M ZnCl_2 in 3 M HCl solution. The phases were separated after the addition of sufficient amount of diluent. To quantify the amount of ether and diluent in the aqueous phase, we used qNMR. To that end, 0.7 mL of each aqueous phase was transferred to separate NMR tubes, and 15–20 mg citric acid was added to each sample as internal calibrant.

Batch extraction

For the batch LLE of gallium, seven centrifuge tubes were charged with 1.3 mL of 5.6 M ZnCl₂ made in 3 M HCl solution, also containing ⁶⁷Ga and ⁶⁵Zn. To this, 3 mL of one of the seven ethers, Et₂O, ⁱPr₂O, THP, Bu₂O, *n*-BuOMe, *n*-HexOMe, or *n*-Am₂O, mixed with TFT (1/2 v/v) was added. The tubes were shaken for 30 minutes, centrifuged at 4000 rpm, and the phases were separated. The activity of ⁶⁷Ga and ⁶⁵Zn in each phase was quantified by gamma spectroscopy. The batch LLEs with all seven ethers with TFT (1/2 v/v) were repeated with a solution of 5.6 M ZnCl₂ made in 6 M HCl. The extraction of Mn and Co were studied using the same procedure, where ⁵⁴Mn and ⁶⁰Co were added to the 5.6 M ZnCl₂ in 3 M HCl solution. Batch LLEs with 1 mL of 1 M ZnCl₂ made in 6 M HCl, also containing ⁶⁷Ga and ⁶⁵Zn radionuclides were also performed under the same conditions and same organic solvent mixtures.

The Ga extraction efficiencies (EE(%)) were calculated from the activities of ⁶⁷Ga in the organic phase divided by the total activities in the aqueous and organic phase as shown in

$$EE(\%) = \frac{{}^{67}\text{Ga}_{org}}{{}^{67}\text{Ga}_{org} + {}^{67}\text{Ga}_{aq}} \times 100\% \quad (1)$$

The Zn extraction was calculated in the same way using the radioactivities of ⁶⁵Zn. The percent Ga recovery and the percent Zn contamination were calculated as the activity of ⁶⁷Ga and ⁶⁵Zn in the 0.1 M HCl stripping solution divided by the activities of the respective radionuclides in the aqueous solution before the extraction and stripping.

Flow extraction

A 3-stage separation of gallium from zinc using liquid-liquid extraction in flow is presented in Figure 2. In stage 1 (extraction), the aqueous feed consisted of a solution of 1 M ZnCl₂ made in 6 M HCl, also containing ⁶⁷Ga and ⁶⁵Zn radionuclides, and the aqueous phase contained a 1/2 (v/v) mixture of *n*-BuOMe/TFT. In stage 2, the 8 M HCl was used as an aqueous phase to selectively remove Zn from the organic phase (scrubbing). In stage 3 radiogallium was back-extracted from the organic into the aqueous phase (stripping). For the purpose of screening and optimization studies, either a single-stage extraction or a double-stage extraction and stripping was used. In these experiments, the aqueous feed consisted of a solution of either 5.6 M ZnCl₂ made in 3 M HCl or a solution of 1 M ZnCl₂ made in 6 M HCl. A 1/2 (v/v) mixture of Et₂O, ⁱPr₂O, THP, *n*-BuOMe, *n*-HexOMe, *n*-Bu₂O, or *n*-Am₂O with TFT was used as the organic phase. The fluidics were driven by two separate syringe pumps equipped with the Hamilton glass syringes, which were filled with the organic (4.5–9 mL) and the aqueous (1.5–3 mL) phases. The aqueous flow rate was 15 mL/h, and the organic flow rate was 45 mL/h for all experiments. The two phases passed through PFA tubing (1/16" OD, 0.03" ID) and combined in a PEEK tee. The phases were mixed by two 10 element PTFE static mixers placed inside a short piece of PFA tubing (1/8" OD, 1/16" ID). The two phases were further mixed in a 108 cm long PFA tubing (1/16" OD, 0.03" ID) mixing loop by steady slug flow and passed into the membrane separator.

The membrane separator with integrated pressure control (SEP-10) is commercially available from Zaiput Flow Technologies and is similar to one described in detail by Adamo et al.^[14] In the membrane separator, the organic phase permeated the hydrophobic membrane (PTFE/PP, 0.2 μm pore size and 139 μm thickness) and passed through the permeate outlet, while the aqueous phase was retained and passed through the retentate outlet (Figure 3). The 0.002" PFA diaphragm in the membrane separator worked as integrated pressure control, and complete phase separation between the aqueous and the organic phase was obtained with the chosen membrane and diaphragm. Samples of the aqueous and the organic phase were collected after the LLE and the activity were measured using gamma spectroscopy.

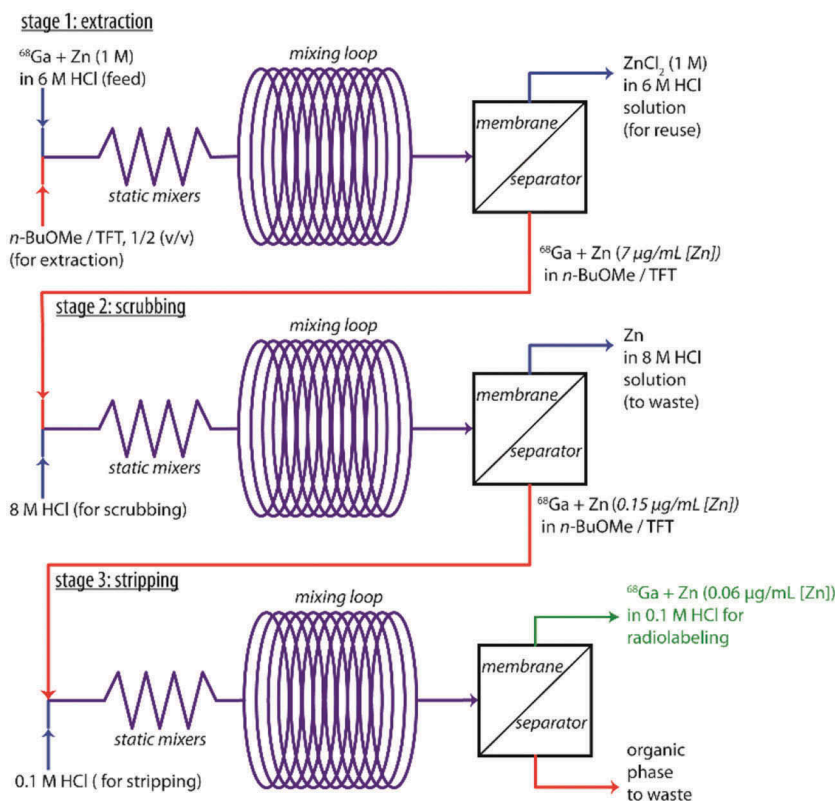


Figure 2. A schematic depicting the liquid-liquid extraction in flow of $^{66,67,68}\text{Ga} = {}^*\text{Ga}$ and Zn using the 1/2 (v/v) mixture of $n\text{-BuOMe}/\text{TFT}$, and hydrochloric acid, also containing 1 M ZnCl_2 , and including scrubbing of residual Zn with 8 M HCl and back-extraction of ${}^*\text{Ga}$ into 0.1 M HCl. The process was performed stepwise.

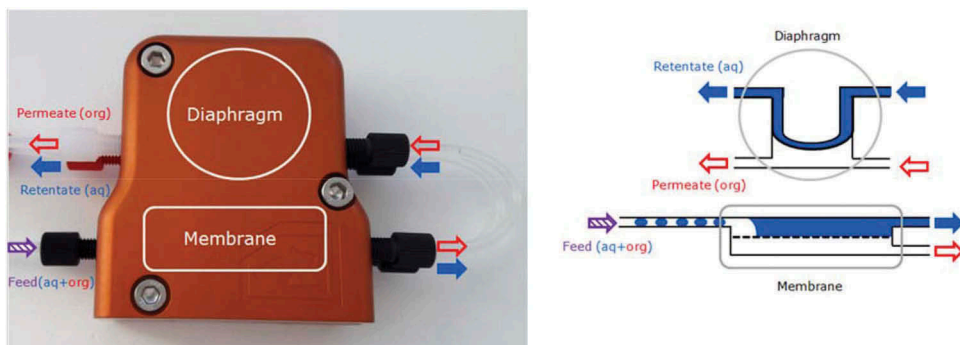


Figure 3. A photograph (left) and a schematic (right) depicting the membrane separator used in this study. The aqueous phase is shown in blue (retained phase) and the organic phase is shown in white (permeated phase).

Fe extraction

The LLE in flow with ${}^i\text{Pr}_2\text{O}/\text{TFT}$ (1/2) as organic phase was repeated, but 9 mM FeCl_3 was added to the 5.6 M ZnCl_2 in 3 M HCl solution. The aqueous phase before and after the LLE was analyzed by ICP-OES.

Copper extraction

7 MBq ^{64}Cu was added to the 5.6 M ZnCl_2 in 3 M HCl solution and the LLE in flow with $^i\text{Pr}_2\text{O}/\text{TFT}$ (1/2) was repeated. The extraction of ^{64}Cu was measured by gamma spectroscopy.

Computational methods

All gas-phase and COSMO calculations were performed using the TURBOMOLE 7.3 suite of programs using the resolution of the identity approximation (RI).^[19] The gas-phase structures were optimized at the RI BP/def2-TZVPD level, and the convergence to the ground state was verified by running analytical frequency calculations. The single-point gas-phase energies were then re-evaluated at the RI MP2/def2-TZVPP level. The COSMO files were obtained at the RI BP/def2-TZVPD level in the COSMO phase with a smooth radii-based isosurface cavity, and the convergence to the ground state was verified by running numerical frequency calculations. The resulting COSMO files were used to perform solution thermodynamics calculations using COSMOtherm, Version C30, Release 18; (COSMOlogic GmbH & Co. KG), yielding the free energies of solvation, sigma surfaces, and sigma profiles.^[20]

Results and discussion

System design

The continuous production of ^{68}Ga necessitates a judicious choice of the chemical composition of the cyclotron target solution and the extraction system. For the radionuclide production, the $^{68}\text{Zn}/\text{Zn}(\text{NO}_3)_2/\text{HNO}_3$ solution has recently become the system of choice over $^{68}\text{Zn}/\text{ZnCl}_2/\text{HCl}$, as HNO_3 reduces pressure buildup during the cyclotron irradiation.^[11] However, when the requirement for the LLE is factored in, a solution based on $^{68}\text{Zn}/\text{ZnCl}_2/\text{HCl}$ appears preferable due to superior extractability of GaCl_3 vs. $\text{Ga}(\text{NO}_3)_3$. ZnCl_2 is also significantly more soluble than $\text{Zn}(\text{NO}_3)_2$ (408 vs. 120 g/100 mL, correspondingly),^[21] which allows one to probe a wider range of zinc concentrations. We considered the composition of the organic phase to be equally important. First and foremost, it should provide for high extractability of ^{68}Ga into the organic phase and excellent ^{68}Ga vs. ^{68}Zn selectivity but at the same time allow for efficient stripping of $^{68}\text{Ga}/\text{GaCl}_3$ back into the aqueous phase. The second critical parameter is the mutual phase contamination, which often occurs during LLE and can be significant at high electrolyte concentrations. A failure to prevent the contamination of the aqueous phase with the organic phase could lead to pressure build-up and soot formation during the cyclotron irradiation of the target solution. Furthermore, the aqueous and organic phases with partial miscibility tend to have low interfacial tension, which might cause a phase breakthrough during the membrane separation step.^[15]

The earlier work established that dialkyl ethers, and in particular Et_2O and $^i\text{Pr}_2\text{O}$, efficiently and selectively extracted gallium from 5–7 M hydrochloric acid solutions in batch.^[18,22–26] In view of the dialkyl ethers being generally nontoxic, readily available, low boiling-point liquids with significant variation in hydrophobicity, we decided to evaluate this class of compounds for further development in LLE and membrane-based separation of Ga from Zn. Since the $^*\text{Ga}$ production yield and its extractability, as well as the $^*\text{Ga}$ vs. Zn selectivity, is expected to depend on zinc and HCl concentrations, we decided to explore both high (5.6 M) and low (1 M) concentrations of ZnCl_2 and HCl (3 M vs. 6 M).

Phase equilibrium at high (5.6 M) ZnCl_2 concentration

THP, Et_2O , *n*-BuOMe, $^i\text{Pr}_2\text{O}$, *n*-HexOMe, *n*-Bu₂O, and *n*-Am₂O ethers were chosen as the extractants. The preliminary experiments showed that the presence of concentrated ZnCl_2

dramatically influenced the equilibrium between the aqueous and organic phases. A single phase was observed by mixing equal volumes of Et₂O and a 5.6 M solution of ZnCl₂ prepared in 6 M HCl. Lowering the concentration of HCl to 5 M, and then to 4 M still produced a single phase. At 3.5 M HCl, two phases finally separated, but extensive migration of aqueous phase into the organic phase was observed (Figure 4 A, circles, green trace) and confirmed by the qNMR. Lowering the concentration of HCl further led to an exponential decrease in $V(\text{Et}_2\text{O})/V(\text{aq})$ and consequently to a decrease in the migration of aqueous phase into the organic phase. Remarkably, this trend was opposite to what was reported in the literature in the absence of ZnCl₂ (Figure 4 A, squares, teal trace).^[18,22] Gratifyingly, the presence of 5.6 M ZnCl₂ had a positive influence on radiogallium extraction. Already at 3 M HCl in the presence of 5.6 M ZnCl₂, 80% of radionuclide could be extracted into Et₂O, whereas without ZnCl₂, the extraction efficiencies in 3 M HCl were reported to be below 20%.^[18] Regrettably, we found that together with the aqueous phase, more than 60% of ZnCl₂ was co-extracted into the organic phase (Figure 4 B). The reason for increased solubility of the 5.6 M ZnCl₂ in the ether phase is unclear at the moment. One can speculate that at high concentrations neutral and mostly covalent oligomeric chains (ZnCl₂-H₂O)_n start to form and migrate into the ether phase.

Encouraged by the medium-to-high levels of radiogallium extraction and the tolerance of cyclotron target to concentrated (5.6–10 M) ZnCl₂ solution reported earlier by Jensen and Clark,^[9] we felt that LLE in flow could be further developed while the unfavorable phase equilibrium and high co-extraction of ZnCl₂ could be combatted with a prudent choice of extractant and diluent. Our strategy was to find a suitable diluent that provided for a reliable phase separation with no or little mutual phase contamination while keeping high gallium extraction efficiency and *Ga vs. Zn selectivity. Given its low capacity to dissolve water,^[27] toluene was initially chosen as a diluent for screening the liquid-liquid phase equilibrium in the series of ethers mixed with 5.6 M ZnCl₂ prepared in 6 M HCl. This strategy proved to be successful: Figure 5 (left Y-axis) shows the amount of toluene that had to be added to suppress the migration of the aqueous phase into the organic phase. THP, together with Et₂O, had the highest affinity for the aqueous phase (log *P* = .95 and 0.87, correspondingly), while *n*-Bu₂O and *n*-Am₂O (log *P* = 2.99 and 3.38, correspondingly) required no or little diluent and could be used neat for extraction. The qNMR of the aqueous phase showed that upon equilibration, less than 10% of the ether migrated into the aqueous phase even for the most hydrophilic ethers (Figure 5, right Y-axis). Next, we optimized the nature of the diluent by screening a series of hydrophobic solvents against THP, chosen to challenge the aqueous/organic phase equilibria as a hydrophilic ether. In a panel of diluents selected from five major classes of organic

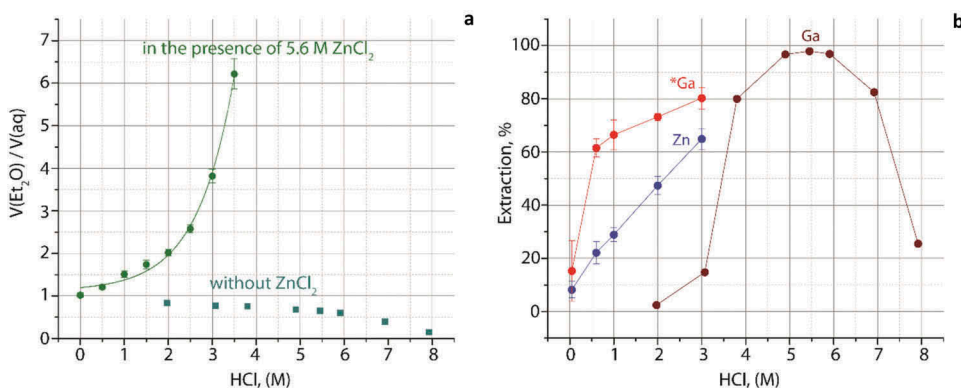


Figure 4. A: Volume changes on equilibrating equal volumes of Et₂O and HCl of various strengths in the presence (5.6 M, circles) and absence (squares) of ZnCl₂. B: Liquid-liquid extraction of radiogallium (^{66,67,68}Ga = *Ga, red) and zinc (⁶⁵Zn, blue) with Et₂O from HCl solutions of various strengths in the presence of 5.6 M ZnCl₂, and the extraction of Ga in the absence of ZnCl₂, as reported by Swift (maroon).^[18] Error bars represent the standard deviation of two consecutive measurements.

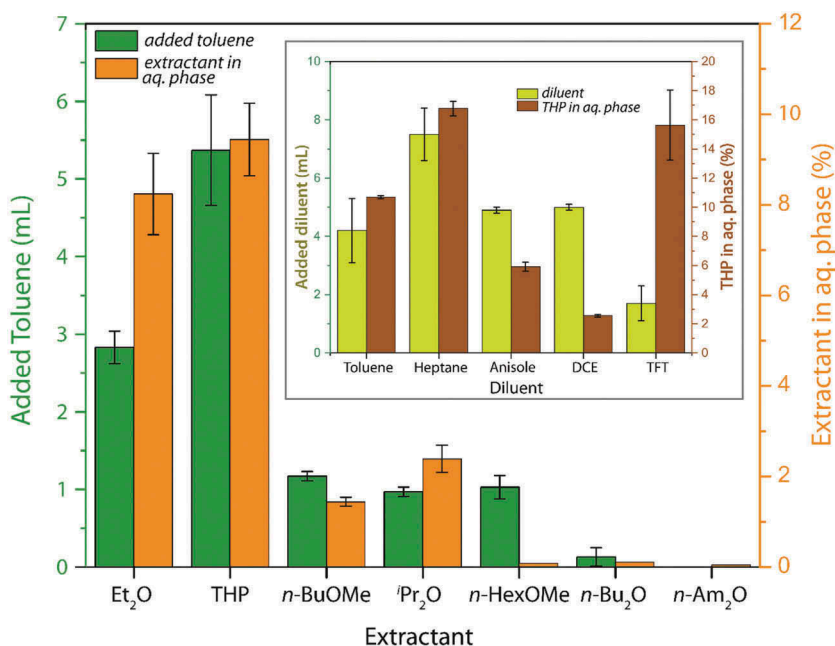


Figure 5. The influence of diluent on the liquid-liquid phase equilibrium containing organic phase and 5.6 M ZnCl₂ prepared in 6 M HCl. Main: The amount of toluene added to the ethereal phase required to reconstitute the initial 1.3 mL of the aqueous phase. Inset: The amount of diluent added to the THP phase required to reconstitute the initial 1.3 mL of the aqueous phase. Error bars represent the standard deviation of two consecutive measurements.

solvents and represented by toluene, anisole, DCE, TFT and heptane, TFT was the most effective, requiring only 1.7 mL to reconstitute the initial 1.3 mL of the aqueous phase (Figure 5, inset, left Y-axis).

Although the amount of THP in the aqueous phase remained substantial at 6 M HCl (Figure 5, inset, right Y-axis), at 3 M HCl it dropped to 4%, suggesting that a judicious choice of the extractant would allow us to further suppress the phase contamination (Fig. S1, Supporting Information).

Batch and in-flow extractions at high (5.6 M) ZnCl₂ concentration

Having established TFT as an optimal diluent, we investigated the ⁶⁷Zn and Zn extractions in batch. At 6 M HCl, a 1/2 (v/v) mixture of TFT and one of the seven ethers in the screening set allowed for radiogallium extraction efficiencies above 80% (Fig. 6, red circles). ⁱPr₂O and n-BuOMe were found to be the best performers extracting up to 97% of radiogallium in 6 M HCl. As expected, the extraction efficiencies decreased in 3 M HCl, with ⁱPr₂O/TFT mixture able to extract 77% of ⁶⁷Zn and 1% of Zn (Fig. 6, red and blue triangles). Only 0.3% of ⁱPr₂O and no TFT was found migrating into the aqueous phase. Among all ethers, THP co-extracted the highest amount of zinc from both 6 M and 3 M HCl.

Next, we translated the batch experiments into fully continuous flow experiments using the apparatus depicted in Figure 2 (single-stage extraction only). The low mutual phase contamination observed in batch at 3 M HCl prompted us to explore LLE in flow of ⁶⁷Zn and Zn from the 5.6 M ZnCl₂/3 M HCl solution using optimized flow conditions established previously.^[15] The organic phase consisted of a 2/1 (v/v) mixture of TFT used as a diluent and Et₂O, THP, ⁱPr₂O, and n-BuOMe used as the extractants. In all cases, clean phase separation was achieved, and the radiogallium was selectively extracted into the organic phase. The organic phase could then be either collected or directly re-routed into the second separation module, where 0.1 M HCl was used as the aqueous phase for stripping. Within the experimental errors, the results of the LLE in flow mirrored those

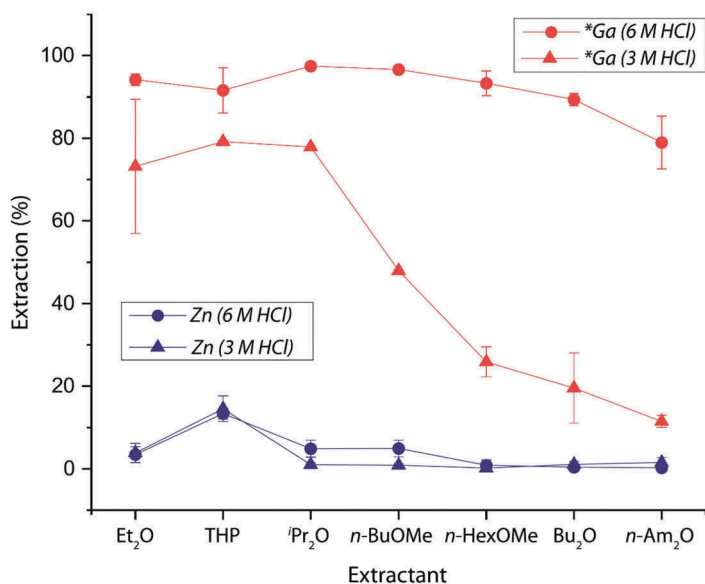


Figure 6. $^{66,67,68}\text{Ga} = {}^*\text{Ga}$ (red, two top traces) and Zn (blue, two bottom traces) extractions in batch using a 1/2, (v/v) mixture of ether/TFT. The aqueous phase is formed by 5.6 M ZnCl_2 prepared either in 6 M HCl (circles) or in 3 M HCl (triangles). Error bars represent the standard deviation of two consecutive measurements.

obtained in the batch experiments: the THP showed the highest radiogallium extraction, but also the lowest ${}^*\text{Ga}$ vs. Zn selectivity (Table 1, entry 2). Measuring the LLE in flow performance over time, we noted that in all cases except *n*-BuOMe (50%), 70% of radiogallium was extracted within the first 2 minutes, and the extraction was complete in under 6 minutes. The ${}^*\text{Ga}$ stripping efficiencies were uniformly high (> 95%) across the series, but little selectivity was observed for ${}^*\text{Ga}$ vs. Zn stripping. For practical implementations, ⁱPr₂O seems to strike the best balance between the levels of radiogallium and zinc extraction.

Batch and in-flow extractions at low (1 M) ZnCl_2 concentration

Turning now to low ZnCl_2 concentration, we found that 1 M ZnCl_2 prepared in 6 M HCl and combined with a 1/2 (v/v) mixture of ether/TFT yielded a well-separated biphasic mixture with no mutual phase contamination. Table 2 shows that ${}^*\text{Ga}$ extractions in batch at 1 M ZnCl_2 were on average on the same level as those obtained from the 5.6 M ZnCl_2 /6 M HCl, but appreciably higher than those obtained from 5.6 M ZnCl_2 /3 M HCl. Importantly, the co-extraction of zinc was one order of magnitude lower for the non-hydrophobic ethers, likely due to increased chloride per zinc equivalents ratio, which promoted the formation of non-extractable ZnCl_4^{2-} [28] (Table 2 entries 1–4).

Table 1. Liquid-liquid extraction and stripping of $^{66,67,68}\text{Ga} = {}^*\text{Ga}$ and Zn in flow using a 1/2 (v/v) mixture of ether/TFT (extraction) and 0.1 M HCl (stripping). The aqueous phase was formed by 5.6 M ZnCl_2 prepared in 3 M HCl. Errors represent the standard deviation of three consecutive measurements.

Entry	Ether	*Ga extraction, %	Zn extraction, %	Ga stripping, %	Zn stripping, %	Ga recovery, %	Zn contamination, %
1	Et ₂ O	81.4 ± 2.6	4.2 ± 0.7	99.7 ± 0.7	91.0 ± 8.2	81.1 ± 2.6	3.8 ± 0.8
2	THP	89.6 ± 3.7	26.2 ± 8.6	99.3 ± 2.8	98.1 ± 4.4	88.9 ± 4.5	25.7 ± 8.5
3	ⁱ Pr ₂ O	76.3 ± 1.9	1.9 ± 1.6	97.8 ± 2.4	93.4 ± 6.3	74.6 ± 2.6	1.7 ± 1.5
4	<i>n</i> -BuOMe	51.8 ± 1.8	2.1 ± 0.3	98.5 ± 3.1	76.5 ± 3.8	51.0 ± 2.4	1.6 ± 0.2

Table 2. Liquid-liquid extraction of $^{66,67,68}\text{Ga} = {}^*\text{Ga}$ and Zn in batch and in flow using a 1/2 (v/v) mixture of ether/TFT. The aqueous phase was formed by 1 M ZnCl_2 prepared in 6 M HCl. Errors represent the standard deviation of two consecutive measurements.

Entry	Extractant	Batch		Flow	
		*Ga %	Zn %	*Ga %	Zn %
1	Et_2O	96.4 ± 1.7	0.3 ± 0.2	98.9 ± 0.2	0.2 ± 0.2
2	THP	98.0 ± 1.1	1.7 ± 0.5	97.4 ± 2.0	1.5 ± 0.5
3	${}^i\text{Pr}_2\text{O}$	93.1 ± 1.1	0.4 ± 0.5	97.5 ± 1.3	0.1 ± 0.1
4	<i>n</i> -BuOMe	98.0 ± 0.4	0.5 ± 0.7	95.7 ± 2.0	$5 \cdot 10^{-3} \pm 3 \cdot 10^{-3}$
5	<i>n</i> -HexOMe	93.9 ± 1.6	0.4 ± 0.2	90.6 ± 3.5	$2 \cdot 10^{-3} \pm 2 \cdot 10^{-4}$
6	Bu_2O	84.8 ± 4.9	0.3 ± 0.2	87.3 ± 0.4	0.01 ± 0.01
7	<i>n</i> -Am $_2\text{O}$	73.6 ± 1.4	0.5 ± 0.1	80.4 ± 1.5	$2 \cdot 10^{-3} \pm 1 \cdot 10^{-3}$

Next, all seven ethers were chosen for translation in flow. Running LLE in flow under the optimized conditions reported in Table 1 resulted in smooth and reproducible phase separation with no phase breakthrough. The radiogallium extractions were complete within 6 minutes, and the yields were consistent with the batch extractions (Table 2).

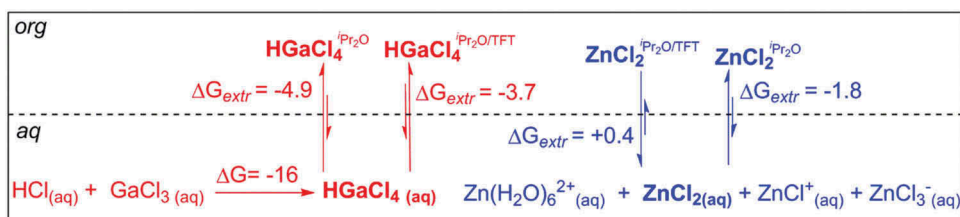
Co-extraction of other metals

Iron is an environmentally ubiquitous metal and is often present as a contaminant during radio-nuclide production. It will also competitively chelate to many gallium chelators.^[29] Therefore, it was important to access the co-extraction of Fe^{III} into the solvent system optimized for the liquid-liquid extraction of gallium. An in-flow extraction of 9 mM FeCl_3 dissolved in 5.6 M ZnCl_2 /3 M HCl with ${}^i\text{Pr}_2\text{O}$ /TFT, 1/2, (v/v) resulted in $66 \pm 2\%$ of Fe extraction into the organic phase and 98% stripping into 0.1 M HCl. The lack of *Ga vs. Fe selectivity demonstrated by our optimized system was not surprising given the high Lewis acidity and strong propensity to form organic-soluble HMCl_4 species by both cations ($M = \text{Ga}, \text{Fe}$).^[30] Small amounts of various chelating Cu, Co, and Mn radionuclidic impurities are also commonly found in the cyclotron-irradiated samples of zinc solutions.^[13] In contrast to Fe extraction, Cu was extracted only at 0.04%, and no detectable extraction was observed for Mn and Co.

COSMO-RS model for extraction of Ga and Zn

Although experimental studies on liquid-liquid extraction of Ga using ethers have a long history, no model explaining equilibrium in the Ga/HCl/ether system has been put forward. An earlier attempt to correlate the extractability of Ga with a dielectric constant of an ether was unsuccessful, and a participation of an extractant in coordination to the metal was conjectured.^[24] A broader question of Ga vs. Zn selectivity arises in the context of LLE of the two metals following cyclotron production of *Ga where the concentrations of HCl and zinc may vary during irradiation due to high temperatures and radiolysis. The speciation of Ga and Zn under different HCl concentrations was studied in detail using titration,^[23,31] X-ray scattering, Raman,^[32] and EXAFS spectroscopy.^[28] These studies provide an opportunity to inform theory about the Ga and Zn species most likely to be present in solution, which coupled with an appropriate computational technique can pave the way to a predictive quantitative model.

The conductor-like screening model for real solvents (COSMO-RS) is one of such computational methodologies. Known for its algorithmic simplicity, numerical stability and robustness COSMO-RS combines first-principle quantum chemistry with statistical thermodynamics. The detailed description of COSMO-RS can be found elsewhere,^[33] but in short, in a first step, a molecule is geometry-optimized in a homogeneous conductor environment yielding the surface polarization charge densities as a molecular descriptor and a measure of a molecular surface polarity. These calculations are performed using density functional theory. In the next step, statistical thermodynamics is used to



Scheme 1. The solution equilibrium for the relevant gallium and zinc species in the aqueous and organic phases as calculated at COSMO-RS-FINE/RI-MP2 level.^[34] The values are in kcal/mol.

quantify intramolecular interaction energies as interactions of polarization charge densities, ultimately yielding chemical potentials of a given species in the system. Thus, COSMO-RS treats a solute and a solvent on the same footing and contains relatively few empirical terms, which allows one to use it outside of parametrization.

Having developed an efficient and reliable experimental method for selective LLE of radiogallium in the presence of zinc, we turned to construct a predictive theoretical model for extraction. The first step was to establish the main extractable species, and these could be gleaned from earlier experimental studies. The works of Reznik and Nachtrieb indicate that in the 3–6 M HCl range, gallium extracts into tributyl phosphate or ${}^i\text{Pr}_2\text{O}$ as a 1/1 mixture of HCl/GaCl₃, presumably in the form of the chlorogallic acid, HGaCl₄.^[23,31] Indeed, we found HGaCl₄ to be a potential-energy minimum in both gas and COSMO phases, and its formation from HCl and GaCl₃ was predicted to go to completion in the aqueous phase ($\Delta G = -16$ kcal/mol, Scheme 1). In line with the experiment, the solution thermodynamics calculations found ${}^i\text{Pr}_2\text{O}$ to be a much better solvent for HGaCl₄ than water, with the difference in the free energy of solvation calculated at -4.9 kcal/mol.

Examination of the COSMO sigma surface of HGaCl₄ reveals that it is dominated by the weakly negatively charged Ga–Cl moieties (Figure 7, yellow-green surface). A better insight into why ${}^i\text{Pr}_2\text{O}$ is an excellent solvent for HGaCl₄ can be obtained by examining their respective sigma profiles, which give a relative amount of surface with a given polarity σ . Figure 7 shows that the weakly negatively charged part of HGaCl₄ represented by peak H is well solvated by a weakly positively charged C–H moieties of ${}^i\text{Pr}_2\text{O}$ (peaks F and G). The positively charged H-atom of HGaCl₄ (peak C) is solvated by the negatively charged O-atom of ${}^i\text{Pr}_2\text{O}$, (peak J). Therefore, the sigma profiles of HGaCl₄ and ${}^i\text{Pr}_2\text{O}$ are complementary, translating into high free energy of solvation ($\Delta G_{\text{solv}} = -9.9$ kcal/mol) and high extractability into the organic phase.

The speciation of the ZnCl₂ solutions is more complex. The previous EXAFS and Raman studies conclude that in 7.5 M solution ZnCl₂ is present as an almost equimolar mixture of Zn(H₂O)₆²⁺, ZnCl₂, ZnCl⁺, and ZnCl₃⁻.^[32] The charged zinc species are not directly extractable into the ether phase, but as a neutral species, ZnCl₂ is expected to be solvated by ${}^i\text{Pr}_2\text{O}$. The examination of ZnCl₂ sigma profile reveals that a substantial part of its negatively charged sigma surface is outside of the main ${}^i\text{Pr}_2\text{O}$ solvation (Figure 7, peak I). Furthermore, the peaks A and B, corresponding to the high-density surface charge around Zn²⁺ have no matching solvent counterparts. Consequently, the transfer of ZnCl₂ from the aqueous into the organic phase is less favorable than for Ga (-1.8 kcal/mol vs. -4.9 kcal/mol), hence lower extraction. As the concentration of external HCl increases, more ZnCl₂ is expected to form, driving higher zinc extraction. This is consistent with our experimental observations, where a significant extractability of Zn into Et₂O was observed at higher acid concentrations (Figure 4 B). The thermodynamics changes when TFT is added to the extractant. While the Ga extraction into the organic phase remains exergonic ($\Delta G_{\text{extr}} = -3.7$ kcal/mol), the Zn extraction becomes endergonic ($\Delta G_{\text{extr}} = +0.4$ kcal/mol) keeping the Zn in the aqueous phase. Thus, the less polar TFT acts not only as a diluent preventing mutual phase contamination and increasing the interfacial tension but also as a metal solvation modulator, leading to increased Ga vs. Zn extraction selectivity. With the COSMO-RS model in hand, we computed the LLE of Ga and Zn under the batch extraction conditions (Figure 8). An excellent agreement with the experiment was achieved for the

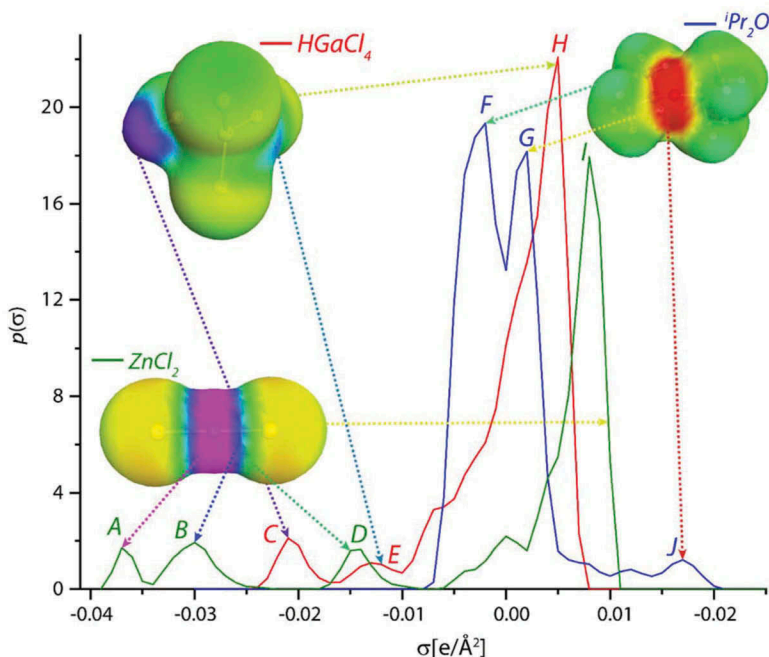


Figure 7. The depiction of COSMO sigma surfaces (polarization charge densities) and sigma profiles for HGaCl_4 , ZnCl_2 , and $i\text{Pr}_2\text{O}$.

extraction of Ga into the C4–C7 ethers measured for both high (5.6 M) and low (1 M) ZnCl_2 concentrations in 6 M HCl as evidenced by a mean unsigned error of prediction (MUE, 2.8% and 4.0% correspondingly). The corresponding MUE for the hydrophobic ethers ($n\text{-Bu}_2\text{O}$ and $n\text{-Am}_2\text{O}$) was somewhat higher at 13.2% and 10.1%.

Experimentally, when 1 M ZnCl_2 was prepared in 6 M HCl, the extraction of zinc was very low (Table 2), which is consistent with its speciation diagram dominated by the non-extractable ZnCl_4^{2-} due to the higher Cl/Zn ratio.^[28] Therefore, the modeling of Zn extraction was performed using high (5.6 M) concentrations, where the presence of neutral ZnCl_2 can be substantial. This yielded the MUE of extraction prediction for Zn at 3.4%, with THP giving the largest error at 7%. It is important to emphasize that while the current modeling efforts considered HCl as a reagent, critical in determining the chemical form of the extracted metal species, its contribution as a solvent was neglected, as no COSMO model for HCl in solution exists. This underscores the importance of developing a COSMO-RS model for concentrated hydrochloric acid, which will help to further improve the quality of predicting the liquid-liquid equilibrium in acidic media.

Advantages, limitations and further development of LLE in flow

Under optimized conditions the LLE in flow is a fast, reproducible and robust operation at both high and low ZnCl_2 concentrations. Preliminary experiments conducted in our laboratory indicate that a cyclotron solution target with niobium body and foil, which was also used by Jensen et al.,^[9] exhibited good corrosion resistance during short (≤ 30 minutes), low current (≤ 10 μA) cyclotron irradiation of both the 5.6 M $\text{ZnCl}_2/3$ M HCl and 1 M $^{68}\text{Zn}/\text{ZnCl}_2/6$ M HCl solutions when running as an open system. The irradiation of the latter solution for 10 min at 10 μA yielded 350 MBq/ μA of activity, which corresponded to a 79% of the theoretical saturation yield as calculated from the experimental cross sections using SRIM software. While both processes can be considered potentially suitable for implementation within the

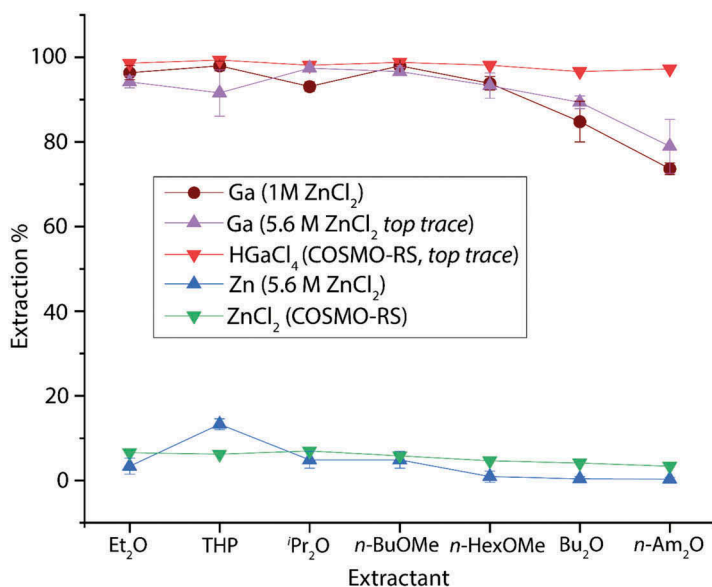


Figure 8. The comparison of experimental (circles and upward triangles) and calculated (downward triangles) extraction of gallium and zinc. The organic phase: 1/2 ⁱPr₂O/TFT, (v/v), the aqueous phase: 5.6 M or 1 M ZnCl₂ in 6 M HCl. The calculations were performed at the COSMO-RS-FINE level of theory.^[33] Error bars represent the standard deviation of two consecutive experimental measurements.

primary recirculation loop, the appreciably higher ⁶⁸Ga and lower Zn extractions from the 1 M [⁶⁸Zn]ZnCl₂/6 M HCl mixture make it a preferred candidate for development. In fact, we showed that when implemented as a single-stage LLE in flow and followed by scrubbing of residual Zn with 8 M HCl and back-extraction of ⁶⁸Ga into 0.1 M HCl, the method could deliver radiogallium in 90% yield and reduce the final zinc contamination to an estimated 0.06 µg/mL, which, at typical ⁶⁸Ga-production yields could meet the current requirements of the European Pharmacopeia monograph^[35] (Figure 2). If required, any additional purification can be performed downstream the primary recirculation loop using one of the SPE-based purification protocols described elsewhere.^[11–13] When compared to the existing methods of ⁶⁸Ga productions using liquid targets, the ability of the continuous process to recycle ⁶⁸Zn on the fly could translate into significant savings. With the current ⁶⁸Zn prices at ~\$1/mg, one can expect to reduce the price of a batch by \$200–\$700. The continuous production also means the process can be stopped and re-started at any time. This could lead to an easy batch size scaling and dose-on-demand production.^[36] On the other hand, one of the challenges inherent to the process is that there will be a limit of how many times the target solution can be recirculated without a significant loss of yield or accumulating too many impurities. Implementation of in flow-compatible PAT tools such as Raman and near infrared spectroscopy would be important, as it could provide critical process understanding and inform the regulators about science and quality risk-based management within the framework of the FDA's Quality-by-Design as applied to continuous production of ⁶⁸Ga.^[37]

Conclusions

In conclusion, we found that radiogallium can be efficiently extracted from ZnCl₂ solutions in batch and in flow using a membrane-based liquid-liquid separator with integrated pressure control. For extractions from concentrated (5.6 M) solutions of ZnCl₂ prepared in 3 M HCl, a 1/2 (v/v) mixture of ⁱPr₂O/TFT is preferred, extracting 76.3 ± 1.9% of radiogallium and 1.9 ± 1.6% of Zn. When 1 M solutions of ZnCl₂ is prepared in 6 M HCl, the extraction of radiogallium and ⁶⁸Ga vs. Zn selectivity

is appreciably higher. In this case, a 1/2 (v/v) mixture of *n*-BuOMe/TFT is the system of choice, extracting $95.7 \pm 2.0\%$ of radiogallium and co-extracting only $0.005 \pm 0.003\%$ of Zn. Trifluorotoluene (TFT) plays a key role in controlling the interfacial tension between the aqueous and the organic phases, and their miscibility, which is critical for successful operation of membrane-based separation of the liquid phases in flow. The COSMO-RS model developed for this system confirms that the ethers act as solvation extractants for the metals and that TFT modulates Ga and Zn solvation, thus increasing the *Ga vs. Zn extraction selectivity. HCl appears to control the speciation of gallium and zinc, and a higher concentration of HCl is beneficial for extraction. Assuming HGaCl_4 and ZnCl_2 to be the species extractable in the organic phase, the COSMO-RS theory predicts the extraction of gallium and zinc with the MUE of prediction at 4.0% and 3.4% respectively. The high efficiency and selectivity of the radiogallium LLE in flow and its compatibility with commercial cyclotron liquid targets encourages further development of the ZnCl_2/HCl -based system, thus paving the way towards fully automated continuous production of ^{68}Ga .

Conflict of Interest

The author declare that there is no conflict of interest regarding the publication of this article.

Funding

The research was supported by the Independent Research Fund Denmark, Grant [8022-00111B].

References

- [1] Bekerman, C.; Hoffer, P. B.; Bitran, J. D. The Role of Gallium-67 in the Clinical Evaluation of Cancer. *Semin. Nucl. Med.* 1984, 14, 296–323. DOI: 10.1016/S0001-2998(84)80005-7.
- [2] Even-Sapir, E.; Israel, O. Gallium-67 Scintigraphy: A Cornerstone in Functional Imaging of Lymphoma. *Eur. J. Nucl. Med. Mol. Imaging.* 2003, 30, S65–S81. DOI: 10.1007/s00259-003-1164-7.
- [3] Vorster, M.; Buscombe, J.; Saad, Z.; Sathekge, M. Past and Future of Ga-citrate for Infection and Inflammation Imaging. *Curr. Pharm. Des.* 2018, 24, 787–794. DOI: 10.2174/1381612824666171129200611.
- [4] Mojtahedi, A.; Thamake, S.; Tworowska, I.; Ranganathan, D.; Delpassand, E. S. The value of ^{68}Ga -DOTATATE PET/CT in diagnosis and management of neuroendocrine tumors compared to current FDA approved imaging modalities: a review of literature. *Am. J. Nucl. Mol. Imaging.* 2014, 4, 426–434.
- [5] Witkowska-Patena, E.; Mazurek, A.; Dziuk, M. ^{68}Ga -PSMA PET/CT imaging in recurrent prostate cancer: Where are we now? *Cent. European J. Urol.* 2017, 70, 37–43.
- [6] Velikyan, I.; ^{68}Ga -based Radiopharmaceuticals: Production and Application Relationship. *Molecules.* 2015, 20, 12913–12943. DOI: 10.3390/molecules200712913.
- [7] Chakravarty, R.; Chakraborty, S.; Ram, R.; Vatsa, R.; Bhusari, P.; Shukla, J.; Mittal, B. R.; Dash, A. Detailed evaluation of different $^{68}\text{Ge}/^{68}\text{Ga}$ generators: an attempt toward achieving efficient ^{68}Ga radiopharmacy. *J. Labelled Compd. Radiopharm.* 2016, 59, 87–94. DOI: 10.1002/jlcr.v59.3.
- [8] Engle, J. W.; Lopez-Rodriguez, V.; Gaspar-Carcamo, R. E.; Valdovinos, H. F.; Valle-Gonzalez, M.; Trejo-Ballado, F.; Severin, G. W.; Barnhart, T. E.; Nickles, R. J.; Avila-Rodriguez, M. A. Very High Specific Activity $^{66}/^{68}\text{Ga}$ from Zinc Targets for PET. *Appl. Radiat. Isot.* 2012, 70, 1792–1796. DOI: 10.1016/j.apradiso.2012.03.030.
- [9] Jensen, M.; Clark, J., in *Proceedings of 13th International Workshop on Targetry and Target Chemistry*, Danmarks Tekniske Universitet, Risø Nationallaboratoriet For Bæredygtig Energi, Denmark. 2011, pp. 288–292.
- [10] Moreira, H. M. R.; Cyclotron Production of ^{68}Ga Using a ^{68}Zn -Based Liquid Target, MSc thesis, University of Coimbra, 2013.
- [11] Pandey, M. K.; Byrne, J. F.; Jiang, H.; Packard, A. B.; DeGrado, T. R. Cyclotron production of ^{68}Ga via the $^{68}\text{Zn}(p,n)^{68}\text{Ga}$ reaction in aqueous solution. *Am. J. Nucl. Mol. Imaging.* 2014, 4, 303–310.
- [12] Alves, V.; Do Carmo, S.; Alves, F.; Abrunhosa, A. Automated Purification of Radiometals Produced by Liquid Targets. *Instruments.* 2018, 2, 17. DOI: 10.3390/instruments2030017.
- [13] Riga, S.; Cicoria, G.; Pancaldi, D.; Zagni, F.; Vichi, S.; Dassenno, M.; Mora, L.; Lodi, F.; Morigi, M. P.; Marengo, M. Production of Ga-68 with a General Electric PETtrace Cyclotron by Liquid Target. *Phys. Med.* 2018, 55, 116–126. DOI: 10.1016/j.ejmp.2018.10.018.

- [14] Adamo, A.; Heider, P. L.; Weeranoppanant, N.; Jensen, K. F. Membrane-Based, Liquid-Liquid Separator with Integrated Pressure Control. *Ind. Eng. Chem. Res.* **2013**, *52*, 10802–10808. DOI: [10.1021/ie401180t](https://doi.org/10.1021/ie401180t).
- [15] Pedersen, K. S.; Imbrogno, J.; Fonslet, J.; Lusardi, M.; Jensen, K. F.; Zhuravlev, F. Liquid-Liquid Extraction in Flow of the Radioisotope Titanium-45 for Positron Emission Tomography Applications. *React. Chem. Eng.* **2018**, *3*, 898–904. DOI: [10.1039/C8RE00175H](https://doi.org/10.1039/C8RE00175H).
- [16] Abiev, R. S.; Dymov, A. V. Modeling the Hydrodynamics of Slug Flow in a Minichannel for Liquid-liquid Two-phase System. *Theor. Found. Chem. Eng.* **2013**, *47*, 299–305. DOI: [10.1134/S0040579513040180](https://doi.org/10.1134/S0040579513040180).
- [17] Pauli, G. F.; Chen, S.-N.; Simmler, C.; Lankin, D. C.; Gödecke, T.; Jaki, B. U.; Friesen, J. B.; McAlpine, J. B.; Napolitano, J. G. Importance of Purity Evaluation and the Potential of Quantitative ¹H NMR as a Purity Assay. *J. Med. Chem.* **2014**, *57*, 9220–9231. DOI: [10.1021/jm401509e](https://doi.org/10.1021/jm401509e).
- [18] Swift, E. H.; A New Method for the Separation of Gallium from Other Elements. *J. Am. Chem. Soc.* **1924**, *46*, 2375–2381. DOI: [10.1021/ja01676a004](https://doi.org/10.1021/ja01676a004).
- [19] *TURBOMOLE V7.3 2018*, a development of University of Karlsruhe and Forschungszentrum Karlsruhe GmbH, 1989–2007, *TURBOMOLE GmbH*, since 2007; available from: <http://www.turbomole.com>.
- [20] Eckert, F.; Klamt, A. Fast Solvent Screening via Quantum Chemistry: COSMO-RS Approach. *AIChE J.* **2002**, *48*, 369–385. DOI: [10.1002/\(ISSN\)1547-5905](https://doi.org/10.1002/(ISSN)1547-5905).
- [21] Lide, D., Ed.. *CRC Handbook of Chemistry and Physics*; CRC Press, United States. **2003**.
- [22] Irving, H. M.; Rossotti, F. J. C. The Solvent Extraction of Group IIIB Metal Halides. *Analyst.* **1952**, *77*, 801–812. DOI: [10.1039/an9527700801](https://doi.org/10.1039/an9527700801).
- [23] Nachtrieb, N. H.; Fryxell, R. E. The Extraction of Gallium Chloride by Isopropyl Ether. *J. Am. Chem. Soc.* **1949**, *71*, 4035–4039. DOI: [10.1021/ja01180a047](https://doi.org/10.1021/ja01180a047).
- [24] Brooks, R. R.; Lloyd, P. J. Influence of Molecular Structure on the Liquid/Liquid Extraction of the Chloro-Complexes of Gallium and Indium with Aliphatic Ethers. *Nature.* **1961**, *189*, 375. DOI: [10.1038/189375a0](https://doi.org/10.1038/189375a0).
- [25] Lewis, M. R.; Reichert, D. E.; Laforest, R.; Margenau, W. H.; Shefer, R. E.; Klinkowstein, R. E.; Hughey, B. J.; Welch, M. J. Production and purification of gallium-66 for preparation of tumor-targeting radiopharmaceuticals. *Nucl. Med. Biol.* **2002**, *29*, 701–706.
- [26] Brown, L. C. Chemical Processing of Cyclotron- Produced ⁶⁷Ga. *Appl. Radiat. Isot.* **1971**, *22*, 710–713. DOI: [10.1016/0020-708X\(71\)90082-2](https://doi.org/10.1016/0020-708X(71)90082-2).
- [27] Kirchnerová, J.; Cave, G. C. B. The Solubility of Water in Low-dielectric Solvents. *Can. J. Chem.* **1976**, *54*, 3909–3916. DOI: [10.1139/v76-562](https://doi.org/10.1139/v76-562).
- [28] D'Angelo, P.; Zitolo, A.; Ceccacci, F.; Caminiti, R.; Aquilanti, G. Structural characterization of zinc(II) chloride in aqueous solution and in the protic ionic liquid ethyl ammonium nitrate by X-ray absorption spectroscopy. *J. Chem. Phys.* **2011**, *135*, 1–7.
- [29] Nurchi, V. M.; Crisponi, G.; Lachowicz, J. I.; Medici, S.; Peana, M.; Zoroddu, M. A. Chemical Features of in Use and in Progress Chelators for Iron Overload. *J. Trace Elem. Med. Biol.* **2016**, *38*, 10–18. DOI: [10.1016/j.jtemb.2016.05.010](https://doi.org/10.1016/j.jtemb.2016.05.010).
- [30] Nachtrieb, N. H.; Conway, J. G. The Extraction of Ferric Chloride by Isopropyl Ether. I. *J. Am. Chem. Soc.* **1948**, *70*, 3547–3552. DOI: [10.1021/ja01191a004](https://doi.org/10.1021/ja01191a004).
- [31] Reznik, A.; Zekel, L. Zh. Tributyl-phosphate extraction of gallium from hydrochloric-acid solutions. *Neorg. Khim.* **1979**, *24*, 1025–1032.
- [32] Maeda, M.; Ito, T.; Hori, M.; Johansson, G. The Structure of Zinc Chloride Complexes in Aqueous Solution. *Z. Naturforsch.* **1996**, *51*, 63–70.
- [33] Klamt, A.; The COSMO and COSMO-RS Solvation Models. *Wiley Interdiscip. Rev. Comput. Mol. Sci.* **2011**, *1*, 699–709. DOI: [10.1002/wcms.56](https://doi.org/10.1002/wcms.56).
- [34] Hellweg, A.; Eckert, F. Brick by brick computation of the Gibbs free energy of reaction in solution using quantum chemistry and COSMO-RS. *AIChE J.* **2017**, *63*, 3944–3954.
- [35] *European Pharmacopoeia 9.0*; Council of Europe, Strasbourg, **2013**, pp 1148–1149.
- [36] Arima, V.; Pascali, G.; Lade, O.; Kretschmer, H. R.; Bernsdorf, I.; Hammond, V.; Watts, P.; De Leonardis, F.; Tarn, M. D.; Pamme, N.; et al. Radiochemistry on chip: towards dose-on-demand synthesis of PET radiopharmaceuticals. *Lab Chip.* **2013**, *13*, 2328–2336. DOI: [10.1039/c3lc50269d](https://doi.org/10.1039/c3lc50269d).
- [37] Yu, L. X.; Amidon, G.; Khan, M. A.; Hoag, S. W.; Polli, J.; Raju, G. K.; Woodcock, J. Understanding Pharmaceutical Quality by Design. *Aaps J.* **2014**, *16*, 771–783. DOI: [10.1208/s12248-014-9598-3](https://doi.org/10.1208/s12248-014-9598-3).